International Journal of Dynamics and Control
https://doi.org/10.1007/s40435-022-00953-1

Exploratory mathematical frameworks and design of control systems for the automation of propofol anesthesia

Temitope A. Oshin[1,2]

Received: 17 January 2022 / Revised: 24 March 2022 / Accepted: 28 March 2022
© The Author(s), under exclusive licence to Springer-Verlag GmbH Germany, part of Springer Nature 2022

Abstract
A variety of automatic control systems are increasingly being deployed to assist clinicians to monitor patient functioning and enhance healthcare delivery during surgical procedures. This article deals with the mathematical design framework of closed-loop infusion schemes for propofol delivery in general anesthesia. The main emphasis of this research series is to come up with a better-performing control system which could handle the clinical concerns of automation-based anesthesia without compromise of safety. Also, the research is geared at studying the performance of these plausible control-based automatic drug infusion patterns in a computer environment prior to actual clinical implementation. The study advances the design of effective model-based predictive control (MPC) strategies familiar to engineers in the process industries, as well as a preliminary design of a proportional–integral–derivative (PID) controller. The consideration of the traditional PID controller is followed by two linear MPC strategies and a nonlinear one. These varieties of closed-loop infusion strategies were designed in order to make well-informed comparison and assessment of the promising method(s) of control for the sought clinical application. The successive linearization technique is being applied in novelty to anesthesia in this work. The results indicate that the MPC controllers show great promise for adoption for automated drug delivery in anesthesia delivering better performance. This sets the pace for future investigations which may assess, via pseudo-clinical in silico studies, the deployment of the controllers.

Keywords Biomedicine · General anesthesia · Propofol · Model predictive control · Drug delivery · Process control · Patient monitoring · Automation

1 Introduction

Advanced controllers have recorded much success in clinical applications in recent times. In diverse application areas such as cancer management, diabetes treatment and drug infusion, engineers have seen their technological tools and basic engineering skills benefiting patients. From the world of man-made machines or chemical plants, control engineering has spread its tentacles to the wards of clinical patients assisting doctors in performing their healthcare duties in a safer fashion. There are a number of these control technologies which have found their way to the forefront of modern medical challenges: Among them is model-based predictive control.

Model predictive control (MPC), reputed to be the most widely used industrial control technology [1], has been introduced in recent years to address the spotted control challenges in anesthesia. The basic concept of MPC is illustrated in Fig. 1. At a present time instant, MPC uses a model to predict the process output to a time distance into the future. Based on the "foreseen future" from the predictions, it then proposes an optimal sequence of input moves that should be taken to drive the process to the desired response. The first move only is implemented and the procedure repeats itself in the next time instant. The sequence of input moves is arrived at by solving an optimization problem which often involves physical constraints imposed by the process.

Anesthesia comprises three components: hypnosis (lack of consciousness), analgesia (lack of pain perception) and

✉ Temitope A. Oshin
temitope.oshin@mavs.uta.edu; oshin.temitope@lmu.edu.ng

[1] Department of Chemical Engineering, College of Engineering, Landmark University, PMB 1001, Omu-Aran, Kwara State, Nigeria

[2] Landmark University SDG 3 Cluster (Good Health and Well-Being), PMB 1001, Omu-Aran, Kwara State, Nigeria

Published online: 28 April 2022

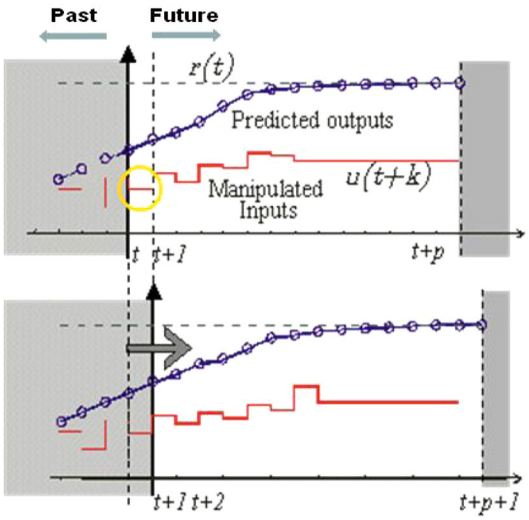

Fig. 1 Model Predictive Control

muscle relaxation (lack of movement). Given the importance and popularity of propofol as an agent of the hypnotic component of anesthesia, designing reliable MPC technologies for its infusion is the major aim of this research. The research's limitation lies in the fact that only the hypnotic component of anesthesia is being considered reducing the control problem to a single-input–single-output (SISO) problem formulation. The effect of the other two components of anesthesia, analgesia and muscle relaxation is not captured. Special emphasis is laid on developing a novel nonlinear MPC strategy (using the successive linearization technique) with the expectation that it could provide better sought-after performance for propofol hypnosis regulation. Therefore, the specific objective pursued is to achieve a comparative evaluation of the nonlinear MPC scheme relative to other control designs including PID and linear MPC. The successive linearization technique is being applied in novelty to anesthesia in this work. This paper covers controller design, tuning and responses.

A number of research teams across the world working on automation in anesthesia have developed and applied various MPC algorithms to propofol anesthesia [2–23]. Although MPC evolved in the 1970s to solve constraints problems in vast petrochemical plants [24], its application to anesthesia is relatively young and developing, being only about two decades old. The age of the application stirs a call for increased involvement in the ongoing improvement of the MPC technology for anesthesia. While the first attempt at achieving automatic control of the depth of anesthesia was made by Bickford in the 1950s [25], it was not until 2000 that the first work on the application of MPC to propofol anesthesia appeared by Rao et al. [12].

It is apparent from these previous works that linear MPC algorithms have been successfully utilized for propofol hypnosis. These linear algorithms use linear internal prediction models of different kinds to achieve control. However, the propofol hypnosis process is intrinsically nonlinear and can be described by a Wiener-type nonlinear model.

Two reasons have made the use of linear predictive models commonly appealing. Firstly, the currently popular MPC algorithms for industrial applications make use of linear models. For example, the dynamic matrix control (DMC) and the model algorithmic control (MAC) employ linear step response and linear impulse response models, respectively. It is easier to adapt these common linear algorithms. More so, their celebrated industrial success has influenced such direct import for propofol hypnosis regulation. The MPC algorithms adopted by Rao et al. (2000) [12] and Yelneedi et al. (2009) [6] each used linear step response models like the DMC.

Secondly, the computational burden often associated with nonlinear algorithms has made linear MPC strategies profuse in comparison with nonlinear MPC approaches. Solving the online optimization problem in a nonlinear MPC algorithm is more computationally expensive. The use of simplified linear models reduces the optimization problem to computationally convenient forms that can be easily handled by conventional optimization solution methods.

However, the use of over-approximated linear predictive algorithms might lead to inaccurate predictions. A marked mismatch between the prediction and the actual patient response often results [6]. Although no model can be truly "perfect" in prediction, closeness to perfection is often a desirable quality, especially for clinical applications. Just as in chemical plants, the process–model mismatch and its resulting safety compromise for clinical patients may portend hazards. A high level of patient safety and non-aggressive drug infusion pattern are sought in anesthesia automation. Both of these standards are at risk in the face of pronounced model inaccuracy. In the MPC algorithm, a large mismatch would lead to an aggressive control action on the drug infusion rate. In a bid to penalize the observed "wide gap" between the prediction and set point, the MPC controller would implement a control action that might be a good deal above that which is actually required. In this paper, effort would be made to design MPC algorithms which would deliver minimal model mismatch in the predictions.

2 Materials and methods

The methodology employed in this research builds on the pharmacokinetic–pharmacodynamic (PK-PD) model of the physiological process to ensure that effective controllers are designed and implemented for onward "pseudo-clinical" (in a virtual non-clinical computer environment) testing. Following the standard procedures for conventional controller designs, this section of the research report first sets out the

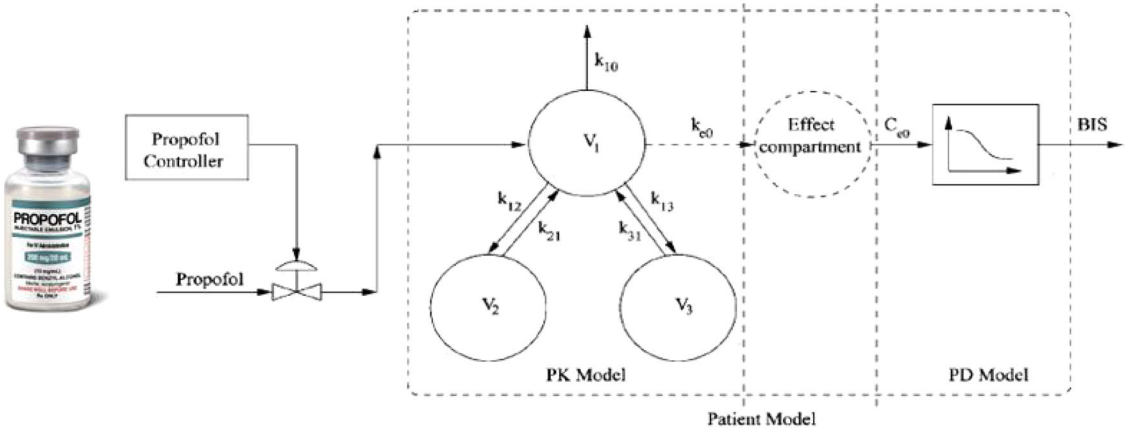

Fig. 2 A schematic of the PK-PD model of propofol hypnosis [6]

clinical problem as a mathematical challenge and articulates the clinical objectives sought. It then outlines the mathematical framework of the advanced control schemes proposed for the regulatory control problem, detailing the internal features peculiar to each one.

2.1 Mathematical model of propofol hypnosis

Although it is acknowledged that the modeling of physiological systems is quite challenging [1], a semiempirical approach has been widely adopted for drug delivery processes. This "gray-box" modeling approach combines the use of a theoretical model proposed from mass balances, with empirical identification of model parameters. The drug mass balances are written based on "compartments" often representing the blood, body or tissues "lumped" into "perfectly mixed volumes" in the same manner that stirred tanks are employed to depict chemical processes. This theoretical modeling paradigm is known as *compartmental modeling*. Standard compartmental models describing the relationship between anesthetic (drug) inputs and patient output indicators (like the bispectral index, BIS) often consists of two interacting parts: a pharmacokinetic (PK) compartment model and a pharmacodynamic (PD) model (Beck et al., 2007) [26]. The model of the BIS response to propofol infusion is a PK-PD model depicted schematically in Fig. 2 [6]. The assessment of hypnotic effect and depth of consciousness are usually derived from the EEG output with a variable known as the bispectral index (BIS). The BIS scale takes numerical value between 0 and 100. A state of full consciousness is indicated by a BIS value of 90–100 while 0 corresponds to a flatline EEG signal.

Pharmacokinetics is the study of the dynamic behavior and distribution of drug concentrations in the blood and tissues [1]. In other words, *pharmacokinetics studies "what the body does to the drug."* PK models predict the disposition and diffusion of drug through conceptual physiological compartments. For the distribution of propofol, three conceptual compartments are used (Fig. 2).

Compartment 1 is the *central compartment* which represents blood plasma. Propofol inflow into the central compartment is considered to be supplied directly by the external intravenous infusion of the drug. After a quick dissolution or mixing of the drug occurs, its concentration in the compartment gradually decreases due to two main sinks: distribution and elimination. The distribution of propofol to the other two compartments results in depletion. Also, propofol leaves the central compartment as a result of metabolic elimination or clearance which occurs in the liver. Compartments 2 and 3 represent shallow and deep peripheral compartments, respectively. Compartment 2 is typically thought of as a group of profusely perfused (vessel-rich) tissues and organs like the brain and muscle [1, 26]. There is a very rapid movement of propofol from the central compartment to this shallow peripheral compartment. It therefore attains steady-state equilibrium quickly. Compartment 3, on the other hand, equilibrates slowly, resulting from a very slow transport of propofol from the central compartment. This deep peripheral compartment typically corresponds to sparsely perfused (vessel-poor) tissues and bone.

Based on Fig. 2, a propofol mass balance in the central compartment is given by:

$$\begin{aligned}\frac{dC_1}{dt} &= \frac{w}{kV_1}u + k_{21}C_2\frac{V_2}{V_1} + k_{31}C_3\frac{V_3}{V_1} \\ &\quad - k_{10}C_1 - k_{12}C_1 - k_{13}C_1\end{aligned} \tag{1}$$

Similarly, for peripheral compartments 2 and 3, the propofol mass balances are given by the following equations.

$$\frac{dC_2}{dt} = k_{12}C_1\frac{V_1}{V_2} - k_{21}C_2 \tag{2}$$

$$\frac{dC_3}{dt} = k_{13}C_1\frac{V_1}{V_3} - k_{31}C_3 \tag{3}$$

V_1, V_2 and V_3 [mL] are the respective volumes of the central compartment, the shallow and the deep peripheral compartments.

C_1, C_2 and C_3 [μg/mL] are the concentrations of propofol in the three pharmacokinetic compartments, respectively.

The constants k_{ij} (k_{12}, k_{21}, k_{13} and k_{31}) refer to the rate constants [min^{-1}] associated with the movement or distribution of the drug from compartment i to j.

k_{10} is the metabolism rate constant depicting the speed of elimination of propofol from the central compartment [min^{-1}].

u [mg/kg-h] is the normalized propofol infusion rate dependent on patient weight, w [kg]. $\bar{k}$, which is equal to 60 [min/h], is a normalization constant.

The depictive coverage of the PK model is limited to the kinetics of elimination and distribution of the drug. In order to reflect the observed clinical effect the drug has on the patient, another set of mathematical description is required. These are known as pharmacodynamic models. Simply put: *pharmacodynamics studies "what the drug does to the body."* PD models therefore seek to relate the drug's concentration in the plasma (central compartment) to the observed clinical effect. For propofol, the site of observed clinical effect is the central nervous system (or chiefly the brain) where loss of consciousness takes effect and the available measurement of this effect is the BIS. In order to develop a PD model for propofol hypnosis, the concentration of propofol in the brain would be needed which is not directly available; it is only accessible in disguise as the BIS signal.

A widely used PD modeling strategy consists of two parts. Firstly, an effect site compartment is attached to the central PK compartment to capture the transport time lag of the drug to the effect site (the brain). This additional compartment allows for the equilibration of the propofol concentrations in the plasma and the brain [1, 6]. This is modeled by a linear first-order ordinary differential equation:

$$\frac{dC_e}{dt} = k_{e0}(C_1 - C_e) \tag{4}$$

where C_e [μg/mL] is the effect site compartment concentration of propofol and k_{e0} [min^{-1}] the associated rate constant for the equilibration taking place in the compartment.

Secondly, an empirical nonlinear static relationship is further used to relate the effect compartment propofol concentration to the observed BIS response. This relation is a sigmoidal function known as the Hill equation. Although the Hill equation is not the only one available to cover and describe the PD term of the PK-PD model as there are a number of Hill and Hill-modified equations, the one often employed for propofol dynamics [6] is presented in Eq. (5).

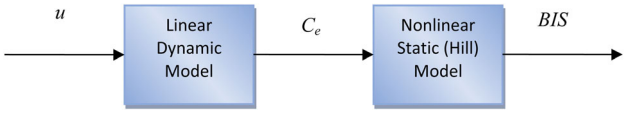

Fig. 3 Wiener-type structure of the propofol hypnosis model

$$\Delta BIS = \Delta BIS_{max}\frac{C_e^{\gamma}}{C_e^{\gamma} + EC_{50}^{\gamma}} \tag{5}$$

where

$$\Delta BIS = BIS - BIS_0 \tag{6}$$

and

$$\Delta BIS_{max} = BIS_{max} - BIS_0 \tag{7}$$

γ is a dimensionless parameter which expresses the degree of nonlinearity of the Hill equation. The EC_{50} [μg/mL] refers to the concentration of the drug which would produce 50% of the maximum PD effect in the patient.

The bispectral index (BIS) is an output measure of the level of hypnosis or unconsciousness of the patient. BIS_0 ($\approx$100) represents the BIS value before the start of propofol infusion when the patient is fully awake while a value of 0 refers to a deep coma state with no electrical brain activity. According to [6], $BIS_{max} = 0$, so that Eq. (7) now becomes

$$\Delta BIS_{max} = -BIS_0 \tag{8}$$

Substituting Eqs. (6) and (8) into (5), Eq. (9) is obtained.

$$BIS = BIS_0\frac{EC_{50}^{\gamma}}{C_e^{\gamma} + EC_{50}^{\gamma}} \tag{9}$$

The PK-PD propofol hypnosis model is a type of Wiener model. A Wiener-type model consists of a linear dynamic part followed in series by a nonlinear static part. The PK component of the model above (Eqs. (1) to (3)) and the first-order time lag Eq. (4) collectively form a system of linear dynamic equations represented by Eq. (10). This is in series with the nonlinear static Hill Eq. (9). Figure 3 depicts this relationship.

Table 1 PK and PD parameters for the nominal patient

Parameter	Value
k_{10} [min^{-1}]	0.119
k_{12} [min^{-1}]	0.112
k_{21} [min^{-1}]	0.055
k_{13} [min^{-1}]	0.0419
k_{31} [min^{-1}]	0.0033
V_1 [mL]	15.048×10^3
V_2 [mL]	30.6×10^3
V_3 [mL]	191.1×10^3
k_{e0} [min^{-1}]	0.349
Γ	2.561
EC_{50} [μg/mL]	2.65

$$\begin{bmatrix} \dot{C}_1 \\ \dot{C}_2 \\ \dot{C}_3 \\ \dot{C}_e \end{bmatrix} = \begin{bmatrix} -(k_{10}+k_{12}+k_{13}) & k_{21}\frac{V_2}{V_1} & k_{31}\frac{V_3}{V_1} & 0 \\ k_{12}\frac{V_1}{V_2} & -k_{21} & 0 & 0 \\ k_{13}\frac{V_1}{V_3} & 0 & -k_{31} & 0 \\ k_{e0} & 0 & 0 & -k_{e0} \end{bmatrix} \begin{bmatrix} C_1 \\ C_2 \\ C_3 \\ C_e \end{bmatrix} + \begin{bmatrix} \frac{w}{kV_1} \\ 0 \\ 0 \\ 0 \end{bmatrix} [u] \tag{10}$$

The propofol hypnosis model has characteristic model parameters which are determined empirically. The PK parameters (k_{10},k_{12}, k_{21},k_{13},k_{31},V_1, V_2 and V_3) are often obtained from clinical population studies. They are dependent on patient mass, height, age and sex [5]. The PD model parameters (k_{e0}, γ, EC_{50}) are also empirically determined.

For a particular 34-year-old patient weighing 66 kg, the PK model parameters have been identified in Table 1 by Marsh et al. (1991) [27]. Included in the table also are the PD model parameters.

2.2 Formulating the control problem

The dynamic action of propofol-induced hypnosis in a clinical patient has been modeled by a set of pharmacokinetic (PK) and pharmacodynamic (PD) Eqs. (10) and (9).

As presented, the model equations represent a single-input–single-output (SISO) control problem with states and output defined as:

$$\mathbf{x} = \begin{bmatrix} C_1 & C_2 & C_3 & C_e \end{bmatrix}^T \tag{11}$$

$$y = [BIS] \tag{12}$$

This representation of states and outputs with conventional algebraic variables would readily transform the patient model to the generic form

$$\dot{\mathbf{x}} = \boldsymbol{A}\mathbf{x} + \boldsymbol{B}u \tag{13}$$

$$y = f(\mathbf{x}) \tag{14}$$

where

$$\boldsymbol{A} = \begin{bmatrix} -(k_{10}+k_{12}+k_{13}) & k_{21}\frac{V_2}{V_1} & k_{31}\frac{V_3}{V_1} & 0 \\ k_{12}\frac{V_1}{V_2} & -k_{21} & 0 & 0 \\ k_{13}\frac{V_1}{V_3} & 0 & -k_{31} & 0 \\ k_{e0} & 0 & 0 & -k_{e0} \end{bmatrix} \tag{15}$$

$$\boldsymbol{B} = \begin{bmatrix} \frac{w}{kV_1} \\ 0 \\ 0 \\ 0 \end{bmatrix} \tag{16}$$

$$f(\mathbf{x}) = BIS_0 \frac{EC_{50}^{\gamma}}{[\boldsymbol{O}_1\mathbf{x}]^{\gamma} + EC_{50}^{\gamma}} \tag{17}$$

$$\boldsymbol{O}_1 = \begin{bmatrix} 0 & 0 & 0 & 1 \end{bmatrix} \tag{18}$$

2.3 Control objectives

It is desirable to achieve a controlled infusion of the anesthetic, propofol, before and during surgery. As earlier dynamic studies have shown [28], this is best achieved in a feedback fashion by allowing the depth of unconsciousness of the patient, as indicated by the bispectral index (BIS), to determine the amount of drug to be administered. Not only does this help achieve a faster induction to "sleep" or unconsciousness, but it represents a good way of ensuring that neither "too much sleep" nor "not enough sleep" results. Both cases, arising from overdosing and underdosing, respectively, are clinical anesthesia crises that must be "controlled." Besides, more demanding requirements arise during surgery when the anesthetists strive to keep the patient unconscious.

The control objectives sought for the problem can be articulated in more specific qualitative and quantitative terms [6]. Firstly, it is desired to track the reference BIS signal as set by the anesthetist and to keep the BIS response in the safe operating range of $40 \leq \text{BIS} \leq 60$ as often as possible. Secondly, it is required to ensure that the plasma propofol concentration C_1 is kept within the clinically acceptable range of $1 \leq C_1 \leq 5$ [μg/mL]. Likewise, it is important to ensure that the delivery of propofol is restricted to the limit $0 \leq u \leq 40$ [mg/kg-h] to avoid hypnotic crisis and to minimize the consumption of propofol. Lastly, it is desirable for the control

system to effectively handle surgical disturbances (stimuli) and measurement noise.

2.4 Steady-state simulation and linearization

Before attempting a dynamic simulation of the nominal patient model, it might be useful to answer the question: "What is the required steady-state propofol infusion rate to maintain a BIS response of 50?" Clinically, a BIS value of 50 is often the desired depth of unconsciousness for anesthesia. Answering that question provides an insight into the operating point at which the anesthesia patient stays induced to unconsciousness.

To achieve this, the time dependencies of the state variables are set to zero:

$$\frac{dC_j}{dt} = 0,\ j = 1, 2, 3, e$$

to obtain the following steady-state relationships:

$$\boldsymbol{C_e^*} = \boldsymbol{EC_{50}}\left(\frac{\mathbf{BIS_0}}{\mathbf{BIS^*}} - 1\right)^{\frac{1}{\gamma}} \tag{19}$$

$$\boldsymbol{C_1^*} = \boldsymbol{C_e^*} \tag{20}$$

$$\boldsymbol{C_2^*} = \frac{\boldsymbol{k_{12}}}{\boldsymbol{k_{21}}}\frac{\boldsymbol{V_1}}{\boldsymbol{V_2}}\boldsymbol{C_1^*} \tag{21}$$

$$\boldsymbol{C_3^*} = \frac{\boldsymbol{k_{13}}}{\boldsymbol{k_{31}}}\frac{\boldsymbol{V_1}}{\boldsymbol{V_3}}\boldsymbol{C_1^*} \tag{22}$$

$$\boldsymbol{u^*} = \frac{\bar{\boldsymbol{k}}\boldsymbol{k_{10}}\boldsymbol{V_1}}{\boldsymbol{w}}\boldsymbol{C_1^*} \tag{23}$$

where the asterisks (*) on the variables denote steady-state conditions.

Using the nominal patient–model parameters given in Table 1, the steady-state concentrations corresponding to $BIS^* = 50$ are

$$C_1^* = C_e^* = 2.65\frac{\mu g}{mL};\ C_2^* = 2.65374\frac{\mu g}{mL};\ C_3^* = 2.6495\frac{\mu g}{mL}$$

The corresponding steady-state propofol infusion rate u^* is

$$u^* = 4.314\frac{mg}{kg.h}$$

It can be observed that the compartment concentrations are roughly equal under steady-state conditions indicating that the anesthetic, propofol, has been evenly distributed and has taken effect around the patient's body to produce the depth of unconsciousness desired. The operating infusion rate needed to achieve this equilibration point at which the patient stays induced to unconsciousness is 4.314 [mg/kg-h]. This steady-state value, although slightly lower, compares agreeably with a reported propofol infusion rate value of 6 mg/kg-h for an adult 70-kg male (Rowe, 1998) [32].

With this operating point, we can linearize the model (Eq. (9) precisely) since the linearized model would be used to design the PID and the linear MPC controllers. Using the Taylor's series expansion of the output variable BIS about the operating point truncated at the second term,

$$f(x) = f(x_0) + f^{'}(x_0)(x - x_0)$$

the following linearized model is obtained:

$$BIS - BIS^* = -\frac{\gamma BIS_0 EC_{50}^{\gamma} C_e^{*\gamma-1}}{\left(C_e^{*\gamma} + EC_{50}^{\gamma}\right)^2}(C_e - C_e^*) \tag{24}$$

In terms of conventional deviation variables notation for states and output, the linearized model is

$$\dot{\mathbf{x}} = \boldsymbol{A}\mathbf{x} + \boldsymbol{B}u$$

$$y = \boldsymbol{C}\mathbf{x} \tag{25}$$

where

$$\boldsymbol{C} = \begin{bmatrix} 0\ 0\ 0\ k_m \end{bmatrix} \tag{26}$$

$$k_m = -\frac{\gamma BIS_0 EC_{50}^{\gamma} C_e^{*\gamma-1}}{\left(C_e^{*\gamma} + EC_{50}^{\gamma}\right)^2} \tag{27}$$

2.5 Design framework for the PID control scheme

The standard proportional–integral–derivative (PID) control scheme was the first closed-loop plan explored for the problem. The PID control law responds to the error difference ϵ in the BIS output signal and the reference or target set for it. It does this in three additive ways: proportionally, integrally and differentially as expressed in Eq. (28).

$$u = K_c\epsilon + \frac{K_c}{\tau_I}\int_0^t \epsilon dt + K_c\tau_D\frac{d\epsilon}{dt} \tag{28}$$

where the parameters K_c, τ_I, τ_D characterize the controller design. The goal of design is to ensure that the values to which they are "tuned" achieve satisfactory control of the process.

There are different tuning strategies, one of the commonest being the Ziegler–Nichols open-loop tuning strategy which was adopted here. For this approach, it is a requirement to obtain a first-order plus time delay approximation of the

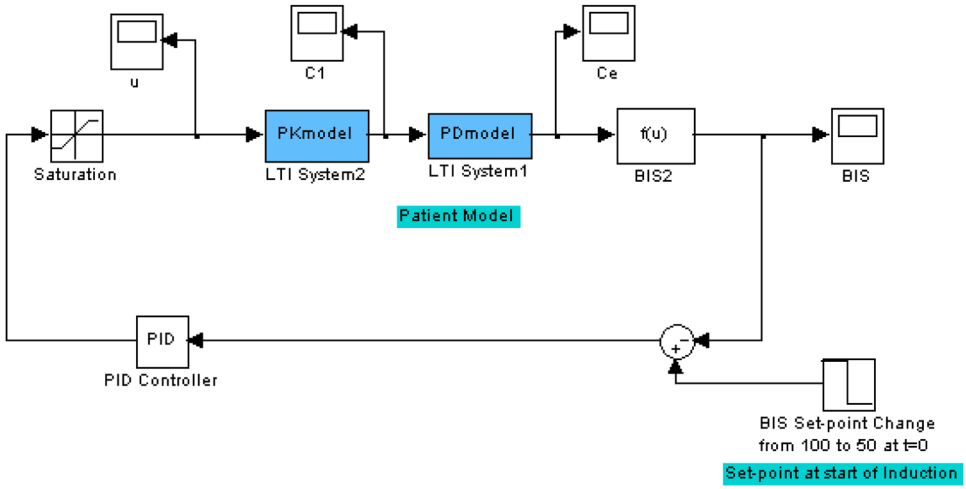

Fig. 4 Closed-loop study of the propofol hypnosis regulation problem with a PID controller

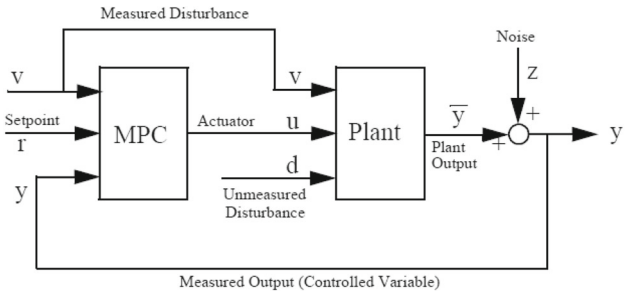

Fig. 5 Block diagram of a SISO MPC Toolbox application reproduced from The MathWorks, 2004 [19]

process. Three parameters which characterize this approximation are the process gain K_p, the first-order time constant τ and the time delay t_d. These parameters were obtained from a process reaction curve (PRC) of the system.

A PRC arising from a unit step input was generated using the linearized model of the nominal patient. It was obtained that $K_p = -14.8178$, $\tau = 21.3068$, and $t_d = 2.1307$. According to the Ziegler–Nichols open-loop tuning guide, the PID settings obtained are: $K_c = -0.8098$, $\tau_I = 4.261$, and $\tau_D = 1.065$.

A fine-tuning was performed in order to minimize propofol consumption and the initial undershoot in the BIS response. This yielded $K_c = -0.710$, $\tau_I = 6.261$, and $\tau_D = 1.065$ as the eventual controller settings. The settings were implemented in the PID closed-loop SIMULINK configuration of the propofol infusion system shown in Fig. 4. A saturation block was introduced to satisfy the propofol input constraint $0 \leq \mathrm{u} \leq 40$ [mg/kg-h].

2.6 The linear model predictive control (toolbox) strategy

The Model Predictive Control (MPC) Toolbox is a commercial software package providing a graphic user interface (GUI) for the design, analysis and implementation of linear MPC controllers [19]. Figure 5 describes the generic single-input–single-output (SISO) plant model structure employed in the toolbox. The "plant" refers to the process to be controlled which, in this case, is the patient.

The formulation employed in the MPC Toolbox, as relevant for this particular application (propofol anesthesia), is described here briefly using the three key elements characterizing any MPC algorithm: prediction model, optimization problem and control law.

The controller uses a linear discrete state-space prediction model of the form:

$$\mathbf{x}(k+1) = \boldsymbol{A_x}\mathbf{x}(k) + \boldsymbol{B_u}u(k) + \boldsymbol{B_d}\mathbf{d}(k) \tag{29}$$

$$y(k) = \boldsymbol{C_x}\mathbf{x}(k) + \boldsymbol{D_d}\mathbf{d}(k) \tag{30}$$

where k stands for the kth sampling time, $\mathbf{x}(k)$ is the internal state vector of the model, $u(k)$ is the manipulated input (propofol infusion rate), $\mathbf{d}(k)$ is the vector of unmeasured disturbances entering the "plant" (patient) and $y(k)$ is the output (BIS). The unmeasured disturbance $\mathbf{d}(k)$ is modeled either as the output of a LTI (linear time-invariant) system driven by a random Gaussian-like noise or as the output of an integrator when considered as steplike. The latter was favored when making specification for design.

Based on the estimation of the states at current sampling instant, k, the MPC controller solves the following optimization problem to determine the control action to take:

$$\min_{\Delta u(k|k),\ldots\Delta u(M-1+k|k),\,\varepsilon} J = \sum_{i=0}^{P-1}\Big\{\left|\lambda_{i+1}^{y}[y(k+i+1|k) - r(k+i+1)]\right|^2 + \left|\lambda_i^{\Delta u}\Delta u(k+i|k)\right|^2 + \left|\lambda_i^{u}\left[u(k+i|k) - u_{t\,\mathrm{arg}\,et}(k+i)\right]\right|^2 + \rho_\varepsilon \varepsilon^2\Big\} \tag{31}$$

subject to

$$
\begin{aligned}
&u_{\min}(i) - \varepsilon V^{u}_{\min}(i) \le u(k+i|k) \le u_{\max}(i) \\
&\quad + \varepsilon V^{u}_{\max}(i) \quad i = 0, \ldots, P-1 \\
&\Delta u_{\min}(i) - \varepsilon V^{\Delta u}_{\min}(i) \le \Delta u(k+i|k) \le \Delta u_{\max}(i) + \varepsilon V^{\Delta u}_{\max}(i) \\
&y_{\min}(i) - \varepsilon V^{y}_{\min}(i) \le y(k+i+1|k) \le y_{\max}(i) + \varepsilon V^{y}_{\max}(i) \\
&\Delta u(k+h|k) = 0, \quad h = M, \ldots, P-1 \\
&\varepsilon \ge 0
\end{aligned} \tag{32}
$$

where the notation "$(k+i|k)$" denotes the predicted value for time instant $k+i$ made at time instant k. λ_i^y, $\lambda_i^{\Delta u}$ and λ_i^u, are nonnegative weights for the output, input rate and input, respectively. Their values are used to indicate which variable is important to the performance index. u_{target} is the set point for the input.

u_{min}, $u_{\max}$, Δu_{min}, $\Delta u_{\max}$, y_{min} and $y_{\max}$ are the lower/upper bounds on the input, input rate and output variables. ε is a slack variable. ρ_ε is a weight on the slack variable to penalize the violation of the constraints. By default,

$$\rho_\varepsilon = 10^5 max\{\lambda_i^y, \lambda_i^{\Delta u}, \lambda_i^u\}$$

V^u_{min}, V^u_{max}, $V^{\Delta u}_{min}$, $V^{\Delta u}_{max}$, V^y_{min} and V^y_{max} are nonnegatives known as equal concern for relaxation (ECR) used to relax the corresponding constraints. The MPC Toolbox controller by default implements hard input constraints and soft output constraints implying $V^u_{min} = V^u_{max} = V^{\Delta u}_{min} = V^{\Delta u}_{max} = 0$ and $V^y_{min} = V^y_{max} = 1$.

P and M are the prediction and control horizons, respectively. P represents the length of time intervals up to which output prediction is made while M indicates the time distance (in intervals) into the future for which manipulated input move is computed to achieve the control objective of tracking the set point.

The control law indicating the input move to make at each time instant is obtained by solving the above-constrained optimization problem—a quadratic programming (QP) problem. Details can be found in [29] for how related QP matrices are generated for the solution.

2.7 Another linear model predictive control strategy

A linear MPC formulation originally developed for an industrial problem in [30] was also applied to the propofol hypnosis regulation problem [28].

Retaining the earlier notations for the states, input and output variables, the following linear discrete-time state-space prediction model is used:

$$\mathbf{x}(k+1) = \boldsymbol{A_x}\mathbf{x}(k) + \boldsymbol{B_u}u(k) \tag{33}$$

$$y(k) = \boldsymbol{C_x}\mathbf{x}(k) + d(k) \tag{34}$$

where $d(k)$ is the virtual disturbance at the current sampling instant k estimated from the difference between the currently sampled output measurement and the output prediction made. This strategy is one of many ways used to account for offset and mismatch in output prediction for improved accuracy. Future virtual disturbances over the prediction horizon $(k+i)\ldots.(k+P)$ are then assumed to be the same as the current virtual disturbance. That is:

$$d(k+i|k) = d(k) = y_m(k) - \boldsymbol{C_x}\mathbf{x}(k) \text{ for } i = 1, \ldots, P \tag{35}$$

where $y_m(k)$ is the current output measurement and the notation "$(k+i|k)$" still denotes the predicted value for time instant $k+i$ made at time instant k.

Equations (33) and (34) can be used recursively to generate the prediction as illustrated below [31].

1. At one time step ahead, $k+1$, the prediction is:

$$
\begin{aligned}
&\mathbf{x}(k+1|k) = \boldsymbol{A_x}\mathbf{x}(k) + \boldsymbol{B_u}u(k); \\
&y(k+1|k) = \boldsymbol{C_x}\mathbf{x}(k+1|k) + d(k)
\end{aligned} \tag{36}
$$

2. At $k+2$, the two-step ahead prediction is:

$$\mathbf{x}(k+2|k) = \boldsymbol{A_x}\mathbf{x}(k+1|k) + \boldsymbol{B_u}u(k+1|k);$$

$$y(k+2|k) = \boldsymbol{C_x}\mathbf{x}(k+2|k) + d(k) \tag{37}$$

Substituting (36) into (37) to eliminate $\mathbf{x}(k+1|k)$,

$$\mathbf{x}(k+2|k) = \boldsymbol{A_x}^2\mathbf{x}(k) + \boldsymbol{A_x}\boldsymbol{B_u}u(k) + \boldsymbol{B_u}u(k+1|k);$$

$$y(k+2|k) = \boldsymbol{C_x}\mathbf{x}(k+2|k) + d(k) \tag{38}$$

3. The prediction at $k+3$, written from the two-step ahead prediction (38) is:

$$
\begin{aligned}
&\mathbf{x}(k+3|k) = \boldsymbol{A_x}^2\mathbf{x}(k+1|k) \\
&\quad + \boldsymbol{A_x}\boldsymbol{B_u}u(k+1|k) + \boldsymbol{B_u}u(k+2|k);
\end{aligned}
$$

$$y(k+3|k) = \boldsymbol{C_x}\mathbf{x}(k+3|k) + d(k) \tag{39}$$

And by substituting (36) to eliminate $\mathbf{x}(k+1|k)$,

$$
\begin{aligned}
&\mathbf{x}(k+3|k) = \boldsymbol{A_x}^3\mathbf{x}(k) + \boldsymbol{A_x}^2\boldsymbol{B_u}u(k) \\
&\quad + \boldsymbol{A_x}\boldsymbol{B_u}u(k+1|k) + \boldsymbol{B_u}u(k+2|k);
\end{aligned}
$$

$$y(k+3|k) = \boldsymbol{C_x}\mathbf{x}(k+3|k) + d(k) \tag{40}$$

4. This recursive prediction can thus be generalized for i steps ahead:

$$\begin{aligned}\mathbf{x}(k+i|k) &= \boldsymbol{A_x}^{i}\mathbf{x}(k) + \boldsymbol{A_x}^{i-1}\boldsymbol{B_u}u(k) \\ &+ \boldsymbol{A_x}^{i-2}\boldsymbol{B_u}u(k+1|k) + \cdots + \boldsymbol{B_u}u(k+i-1|k);\end{aligned}$$

$$\begin{aligned}y(k+i|k) &= \boldsymbol{C_x}\Big[\boldsymbol{A_x}^{i}\mathbf{x}(k) + \boldsymbol{A_x}^{i-1}\boldsymbol{B_u}u(k) \\ &+ \boldsymbol{A_x}^{i-2}\boldsymbol{B_u}u(k+1|k) + \cdots + \boldsymbol{B_u}u(k+i-1|k)\Big] + d(k)\end{aligned} \tag{41}$$

In vector–matrix compact notation, the future prediction up to the horizon P is given by

$$\boldsymbol{Y} = \boldsymbol{\Psi}\mathbf{x}(k) + \boldsymbol{\Phi}\boldsymbol{U} + \boldsymbol{L}d(k) \tag{42}$$

where

$$\boldsymbol{Y} = \Big[\, y(k+1|k) \ \ldots \ y(k+P|k) \,\Big]^T \tag{43}$$

$$\boldsymbol{U} = \Big[\, u(k) \ \ldots \ u(k+M-1|k) \,\Big]^T \tag{44}$$

$$\boldsymbol{L} = \Big[\, 1 \ \ldots \ 1 \,\Big]^{\boldsymbol{T}} \tag{45}$$

M is the control horizon up to which the optimal input moves are estimated. From M and beyond, the input moves are kept constant in the prediction.

$$u(k+h|k) = u(k+M-1|k),\ h = M,\ \ldots,\ P-1 \tag{46}$$

$$\boldsymbol{\Phi} = \begin{bmatrix} \boldsymbol{C_x B_u} & 0 & \cdots & 0 \\ \boldsymbol{C_x A_x B_u} & \boldsymbol{C_x B_u} & \cdots & 0 \\ \vdots & \vdots & \cdots & \vdots \\ \boldsymbol{C_x A_x}^{P-1}\boldsymbol{B_u} & \boldsymbol{C_x A_x}^{P-2}\boldsymbol{B_u} & \cdots & \sum_{i=M}^{P}\boldsymbol{C_x A_x}^{P-i}\boldsymbol{B_u} \end{bmatrix} \tag{47}$$

$$\boldsymbol{\Psi} = \begin{bmatrix} \boldsymbol{C_x A_x} \\ \boldsymbol{C_x A_x}^{2} \\ \vdots \\ \boldsymbol{C_x A_x}^{P} \end{bmatrix} \tag{48}$$

The optimization problem seeks to minimize the deviations of the output predictions and input from their respective set points. While the output reference or set point $r(k+i)$ is externally supplied, the input reference is internally defined by

$$u_r(k) = \boldsymbol{H}_0(y(k) - d(k)) \tag{49}$$

where

$$\boldsymbol{H}_0 = \boldsymbol{C_x}(\boldsymbol{I} - \boldsymbol{A_x})^{-1}\boldsymbol{B_u} \tag{50}$$

The optimization problem is

$$\begin{aligned}&\min_{u(k|k),\ldots u(M-1+k|k)} J \\ &= 0.5\sum_{i=0}^{P-1}\lambda_{i+1}^{y}[y(k+i+1|k) - r(k+i+1)]^2 \\ &+ 0.5\sum_{i=0}^{M-1}\lambda_{i+1}^{u}[u(k+i|k) - u_r(k+i)]^2\end{aligned} \tag{51}$$

subject to

$$u_{min} \le u(k+i|k) \le u_{\max};\ i = 0,\ \ldots,\ M-1 \tag{52}$$

By defining the input and output reference vectors as

$$\boldsymbol{Y_r} = \Big[\, r(k+1|k) \ \ldots \ r(k+P|k) \,\Big]^T \tag{53}$$

$$\boldsymbol{U_r} = \Big[\, u_r(k) \ \ldots \ u_r(k+M-1) \,\Big]^T \tag{54}$$

The input reference vector computation follows from (49) as

$$\boldsymbol{U_r} = \boldsymbol{H}(\boldsymbol{Y_r} - \boldsymbol{L}d(k)) \tag{55}$$

where

$$\boldsymbol{H} = \begin{bmatrix} \boldsymbol{H}_0 & 0 & \cdots & 0\,0\cdots 0 \\ 0 & \boldsymbol{H}_0 & \cdots & 0\,0\cdots 0 \\ \vdots & \vdots & \cdots & \vdots\vdots\cdots\vdots \\ 0 & 0 & \cdots & \boldsymbol{H}_0\,0\cdots 0 \end{bmatrix} \tag{56}$$

The optimization problem (51) can therefore be alternatively written in vector–matrix form (57) with the constraint (52) remaining valid.

$$\begin{aligned}\min_{\boldsymbol{U}} J &= 0.5(\boldsymbol{Y} - \boldsymbol{Y_r})^T\boldsymbol{Q}(\boldsymbol{Y} - \boldsymbol{Y_r}) \\ &+ 0.5(\boldsymbol{U} - \boldsymbol{U_r})^T\boldsymbol{R}(\boldsymbol{U} - \boldsymbol{U_r})\end{aligned} \tag{57}$$

where the output and input weighting matrices are diagonal matrices defined as

$$\boldsymbol{Q} = \begin{bmatrix} \lambda_1^{y} & \cdots & 0 \\ \vdots & \ddots & \vdots \\ 0 & \cdots & \lambda_P^{y} \end{bmatrix} \tag{58}$$

$$\boldsymbol{R} = \begin{bmatrix} \lambda_1^u & \cdots & 0 \\ \vdots & \ddots & \vdots \\ 0 & \cdots & \lambda_M^u \end{bmatrix} \tag{59}$$

with the use of Eq. (42), the optimization problem can be recast to conform to the standard quadratic programming (QP) problem

$$\min_{\boldsymbol{U}} J = 0.5\boldsymbol{U}^T\boldsymbol{S}\boldsymbol{U} + \boldsymbol{U}^T(\boldsymbol{X}_1\mathbf{x}(k) - \boldsymbol{X}_2(\boldsymbol{Y}_r - \boldsymbol{L}d(k))) \tag{60}$$

subject to

$$\boldsymbol{U} \leq \overline{\boldsymbol{U}}; -\boldsymbol{U} \leq \underline{\boldsymbol{U}} \tag{61}$$

where

$$\boldsymbol{S} = \boldsymbol{\Phi}^T\boldsymbol{Q}\boldsymbol{\Phi} + \boldsymbol{R} \tag{62}$$

$$\boldsymbol{X}_1 = \boldsymbol{\Phi}^T\boldsymbol{Q}\boldsymbol{\Psi} \tag{63}$$

$$\boldsymbol{X}_2 = \boldsymbol{\Phi}^T\boldsymbol{Q} + \boldsymbol{R}\boldsymbol{H} \tag{64}$$

$$\overline{\boldsymbol{U}} = \begin{bmatrix} u_{max} \ \ldots \ u_{max} \end{bmatrix}^T \tag{65}$$

$$\underline{\boldsymbol{U}} = \begin{bmatrix} u_{min} \ \ldots \ u_{min} \end{bmatrix}^T \tag{66}$$

The first row of the optimal solution $\boldsymbol{U}$ obtained from the optimization problem (60), (61) defines the current manipulated input move (propofol infusion rate) to be applied to the process (patient). This is the reason MPC is often regarded as *receding horizon control* because only the first optimal move of the lot computed over the control horizon M is implemented.

For the unconstrained problem, the optimal solution is obtained analytically as

$$\boldsymbol{U} = -\boldsymbol{K}_1\mathbf{x}(k) + \boldsymbol{K}_2(y_r - d(k)) \tag{67}$$

where

$$\boldsymbol{K}_1 = \boldsymbol{S}^{-1}\boldsymbol{X}_1 \tag{68}$$

$$\boldsymbol{K}_2 = \boldsymbol{S}^{-1}\boldsymbol{X}_2 \tag{69}$$

2.8 The nonlinear MPC strategy

The adapted nonlinear MPC strategy for Wiener-type nonlinear models which essentially take advantage of the relative ease of linear MPC uses a local linearization of the nonlinear static component of the Wiener model at every time instant about the current state resulting in the use of a time-varying linear state-space prediction model. It is a successive linearization technique and is being deployed for anesthesia application in novelty.

The same predictive control algorithm which was utilized for the second linear MPC controller holds true here. However, the future output prediction over the prediction horizon P is obtained from the local successive linearization at the current time step k.

To obtain the future predictions, a Taylor series approximation of the nonlinear sigmoidal Hill model of Eq. (17) truncated at the linear term is obtained

$$y(k+i|k) \cong f(\mathbf{x})|_{\mathbf{x}=\mathbf{x}(k)} + \left.\frac{\partial f(\mathbf{x})}{\partial \mathbf{x}}\right|_{\mathbf{x}=\mathbf{x}(k)} [\mathbf{x}(k+i|k) - \mathbf{x}(k)]$$

$$y(k+i|k) \cong n_k + \boldsymbol{C}_{\boldsymbol{x}}\mathbf{x}(k+i|k) \tag{70}$$

where

$$n_k = f(\mathbf{x})|_{\mathbf{x}=\mathbf{x}(k)} - \boldsymbol{C}_{\boldsymbol{x}}\mathbf{x}(k)$$

$$\boldsymbol{C}_{\boldsymbol{x}} = \left.\frac{\partial f(\mathbf{x})}{\partial \mathbf{x}}\right|_{\mathbf{x}=\mathbf{x}(k)} = \frac{-\gamma BIS_0 EC_{50}^{\gamma}[\boldsymbol{O}_1\mathbf{x}(k)]^{\gamma-1}}{\left([\boldsymbol{O}_1\mathbf{x}(k)]^{\gamma} + EC_{50}^{\gamma}\right)^2} \cdot \boldsymbol{O}_1 \tag{71}$$

while the generic form of prediction model (33), (34) employed in the last section still applies, the matrix $\boldsymbol{C}_{\boldsymbol{x}}$ ceases to be constant, but is now dependent on current state estimation $\mathbf{x}(k)$. It should be also noted that the term n_k becomes absorbed in the virtual disturbance which is still validly defined as

$$d(k+i|k) = d(k) = y_m(k) - \boldsymbol{C}_{\boldsymbol{x}}\mathbf{x}(k) \text{ for } i = 1, \ldots, P$$

The rest of the optimization problem formulation and control law are as presented above for the second linear MPC.

3 Results and discussions

3.1 PID design implementation

The response produced by the PID controller is depicted in Fig. 6 for the controlled output BIS, the plasma concentration C_1 and propofol infusion rate. The response was for a BIS set point change from 100 to 50 at the start of anesthesia.

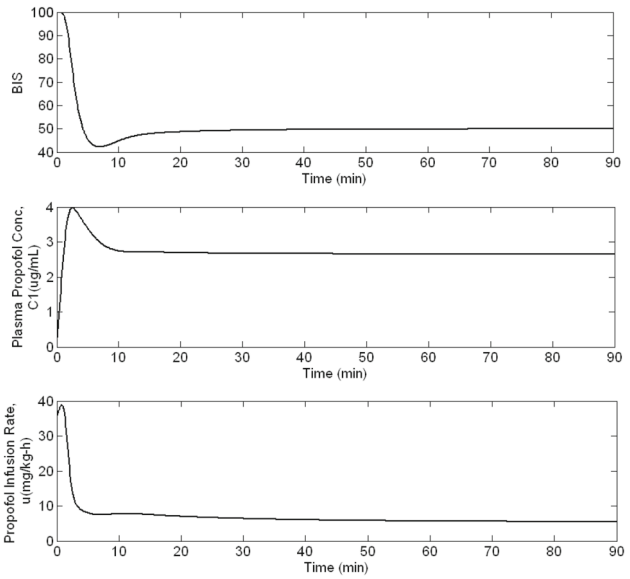

Fig. 6 PID performance for BIS, C_1 and u during the induction phase

This is typical of the clinical practice where the goal is to take the patient to a desired level of unconsciousness (BIS = 50) from his initial fully conscious (BIS = 100) state at the start of administration of propofol. This is the induction stage of anesthesia.

3.2 Implementation, results and discussions of the linear MPC toolbox controller

The LMPC controller design with the MPC Toolbox was initially performed offline employing the "plant" model using different scenarios to judge performance. The toolbox provides interactive interfaces to upload the model, to design a controller and to test it for scenarios of interest. Thereafter, fine-tuning online is performed with the actual process.

The linear continuous model of the nominal patient was supplied to the toolbox. The toolbox would obtain the discrete form from it using the sampling time, T_s provided for the controller. A sampling time of 0.1[min] was adopted. The tuning weights used were: $\lambda_i^y = 1.0$ for the output and $\lambda_i^{\Delta u} = 0.1$ for the input rate. No weight was supplied for the input (that is, $\lambda_i^u = 0$) as there was no desire to penalize its deviation from a predetermined target u_{target}. In addition, an overall weight tuning of 0.5 on a scale of [0, 1] was preferred. This represents halfway between robustness and faster response. Further specifications were made to the controller to enable it model output disturbance and noise effects. Output disturbance and noise of step and white types were selected, respectively, each of magnitude 10.

A prediction horizon $P = 30$ was found to be minimally adequate to improve predictive control action. On the other hand, the control horizon M was tuned to a value of 2. These were obtained from fine-tuning with the nominal "patient" online.

3.3 Implementation and design results for the second linear MPC controller

The above MPC strategy was incorporated in the SIMULINK model of the patient using an s-function block. As was used in the MPC Toolbox controller, the linear continuous state-space model of Eq. (12) was discretized to obtain the discrete state-space matrices $\boldsymbol{A_x}$, $\boldsymbol{B_u}$, $\boldsymbol{C_x}$ which formed part of the input parameters of the s-function block. The rest of the input parameters were the tuning weights $\boldsymbol{Q}, \boldsymbol{R}$ and the horizons P and M. A sample time of 0.1 min was also maintained. The satisfactory prediction and control horizons were obtained to be $P = 30$, $M = 2$. The output and input weights were kept uniform over the respective horizons ($\boldsymbol{Q} = \lambda_i^y \boldsymbol{I}; = \lambda_i^u \boldsymbol{I}$) and tuned as $\lambda_i^y = 1.0, \lambda_i^u = 0.1$. The tuning was performed with the nominal patient online, as was the practice for the earlier controllers.

3.4 Implementation and design results for the nonlinear MPC controller

Again, an s-function block was used to apply the controller; it was coupled with the SIMULINK patient model. The changing $\boldsymbol{C_x}$ at every time step implied the re-computation of the prediction matrices to arrive at the final controller gains utilized in the unconstrained control law. Further, $\boldsymbol{C_x}$ was kept in check in order to avert mathematical and computational errors involved with matrix factorization, especially at the initial stages when it approaches a null matrix. Online tuning of parameters with the nominal patient yielded: the prediction horizons $P = 30$, $M = 2$; the output and input weights $\lambda_i^y = 1.0$, $\lambda_i^u = 0.1$. Figure 7 shows the response generated with the controller over a 30-min induction simulation on the same axes as the previous three controllers.

3.5 Comparative study over the induction phase

In this article, the designs of four closed-loop systems for propofol anesthesia have been examined. In addition to a PID controller which was tuned by the conventional process reaction curve method, two linear model predictive controllers were also designed: one by the MATLAB MPC Toolbox and the other by an s-function block code. Further, a nonlinear model predictive control algorithm was applied, in novelty, to the anesthesia problem. All four controllers have three or four main tuning parameters as summarized in Table 2 and were implemented in SIMULINK where the virtual anesthesia patient model is built.

Induction is the first phase of anesthesia covering the period when the patient starts receiving the anesthetic to the

Table 2 Summary of the controllers' tuning settings

Controller	Main tuning parameters and final settings			
PID	$K_c = -0.710$	$\tau_I = 6.261$	$\tau_D = 1.065$	
LMPC (Toolbox)	$P = 30$	$M = 2$	$Q = 1.0$	$R = 0.1$
LMPC 2	$P = 30$	$M = 2$	$Q = 1.0$	$R = 0.1$
NMPC	$P = 30$	$M = 2$	$Q = 1.0$	$R = 0.1$

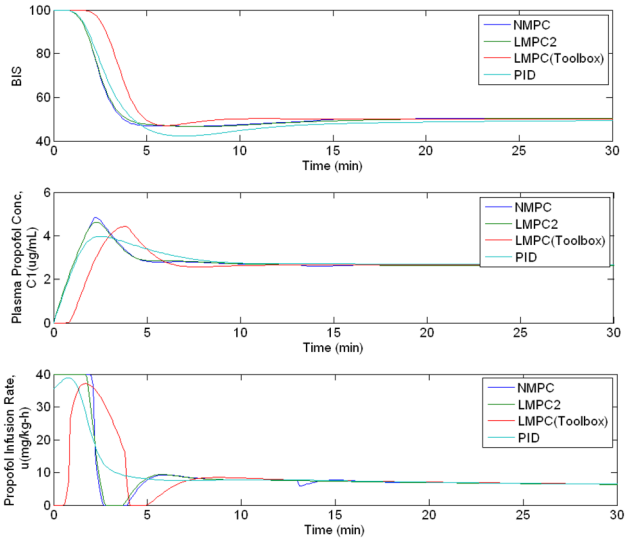

Fig. 7 Comparative performance of all four controllers during the induction phase

time when unconsciousness is achieved. Two key objectives would warrant a special focus on the induction performance of the controllers [8]. Firstly, the target hypnotic level (in this case, BIS = 50) should be attained as fast as possible, with minimal undershoot. Secondly, the closed-loop infusion system should robustly handle the variations existing in patient conditions and parameters without compromising patient safety.

A list of 17 patient sets, adopted from [6], is shown in Table 3 representing a broad range of patient sensitivities. The list of patient variants was generated from the nominal patient (8th patient) by observing changes in PK and PD parameters over three levels of parameter variation: minimum, average and maximum. The list was utilized to vary the parametric conditions of the anesthesia patient for the patient–model mismatch study.

The induction phase was simulated by a step change in BIS from 100 to 50 at the beginning of simulation. All the four closed-loop systems were subjected to this condition. It is worth mentioning again that all the controllers were designed and tuned with the nominal patient (patient 8) model. For each closed-loop system, the anesthesia subject or patient was changed, in succession, while the controller settings remained unchanged until all 17 patient conditions in Table 3 have been used.

Figure 8 shows the responses produced by the PID controller for the 17 patient sets. The swiftness of the BIS responses as well as the initial undershoot varies with the changing patient conditions even as all patients appear to settle to the set point about 40 min into the induction. From this figure, it can be observed that patient 1 was most swift or sensitive in response while patient 17 was the slowest to respond. The most undershoot was experienced with patients 14, 15 and 13 in that decreasing order. All three responses had BIS undershoot below the lower safe limit of 40 by more than 4.5 units over a longer period of time than the others. This is easily attributable to the mismatches existing in the actual patient condition and the controller modeling. Similar BIS responses generated for the model predictive controllers (see Figs. 9, 10 and 11) also show certain patient sets with undershoot responses much below the lower safe limit of 40. While patients 3, 1, 4 and 14 experienced the most undershoot for the MPC Toolbox controller, it was 3, 4 and 14 for the second LMPC strategy and the NMPC controller. In spite of the patient–model mismatches, the controllers were still able to drive all the patients to the set point. LMPC2 and NMPC controllers produced similar profiles for most of the inter-patient variability largely due to the similar mathematical structure of their design algorithm. However, obvious distinctions still exist in their performances with both showing a promising performance.

3.6 Quantitative comparison using performance indices

To enable effective comparison of the responses produced by the controllers, it is necessary to utilize some quantitative criteria for the evaluation of the output and input performance.

3.7 Integral of the absolute error (IAE)

A conventional measure of output control performance known as the IAE (integral of the absolute error) would be utilized as a major performance measure.

Table 3 Parameter values for 17 patient sets [6]

Patient number	Parameter							
	k_{10} [min^{-1}]	k_{12} [min^{-1}]	k_{21} [min^{-1}]	k_{13} [min^{-1}]	k_{31} [min^{-1}]	k_{e0} [min^{-1}]	EC_{50} [μg/mL]	γ
1 (sensitive)	0.08925	0.084	0.06875	0.031425	0.004125	0.459	1.6	2
2	0.14875	0.14	0.04125	0.052375	0.004125	0.239	1.6	2
3	0.14875	0.112	0.04125	0.0419	0.004125	0.239	1.6	3.122
4	0.14875	0.14	0.04125	0.052375	0.004125	0.239	1.6	3.122
5	0.08925	0.084	0.04125	0.052375	0.002475	0.459	2.65	2.561
6	0.08925	0.084	0.06875	0.031425	0.002475	0.349	2.65	2.561
7	0.14875	0.112	0.06875	0.031425	0.002475	0.459	2.65	2.561
8 (nominal)	0.119	0.112	0.055	0.0419	0.0033	0.349	2.65	2.561
9	0.119	0.112	0.055	0.0419	0.0033	0.239	2.65	2
10	0.119	0.112	0.055	0.0419	0.0033	0.239	2.65	2.561
11	0.08925	0.084	0.06875	0.031425	0.002475	0.459	3.7	2
12	0.14875	0.112	0.06875	0.031425	0.002475	0.349	3.7	2.561
13	0.08925	0.084	0.06875	0.031425	0.002475	0.239	3.7	2.561
14	0.08925	0.084	0.06875	0.031425	0.002475	0.239	3.7	3.122
15	0.08925	0.084	0.04125	0.052375	0.002475	0.239	3.7	3.122
16	0.14875	0.14	0.04125	0.052375	0.004125	0.349	3.7	2.561
17(insensitive)	0.14875	0.14	0.04125	0.052375	0.002475	0.239	3.7	3.122

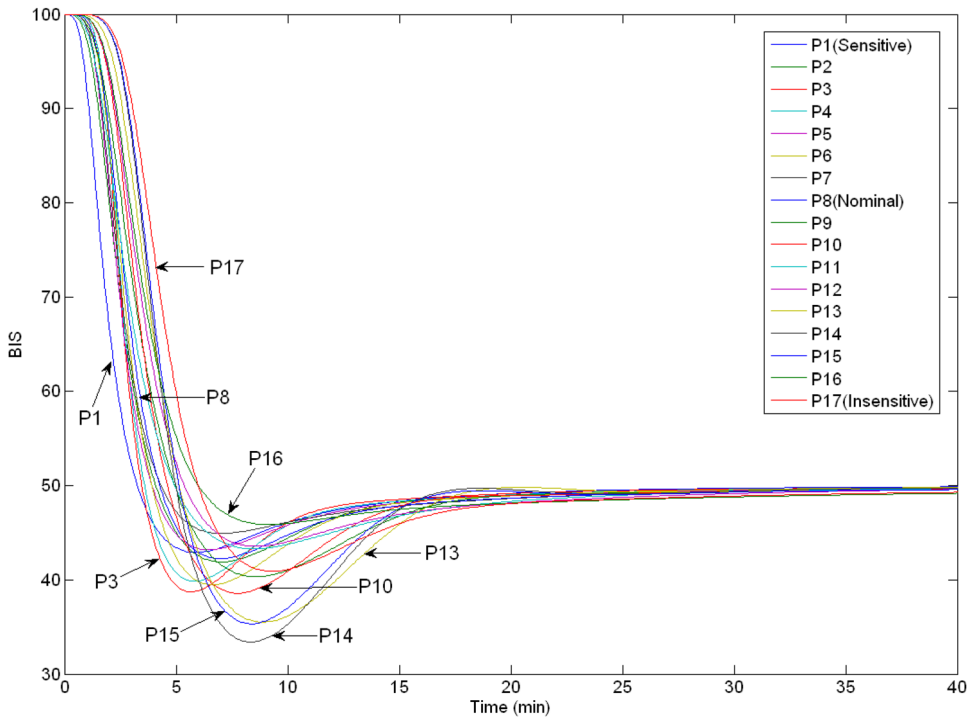

Fig. 8 BIS response with the PID controller 40 min into the induction test

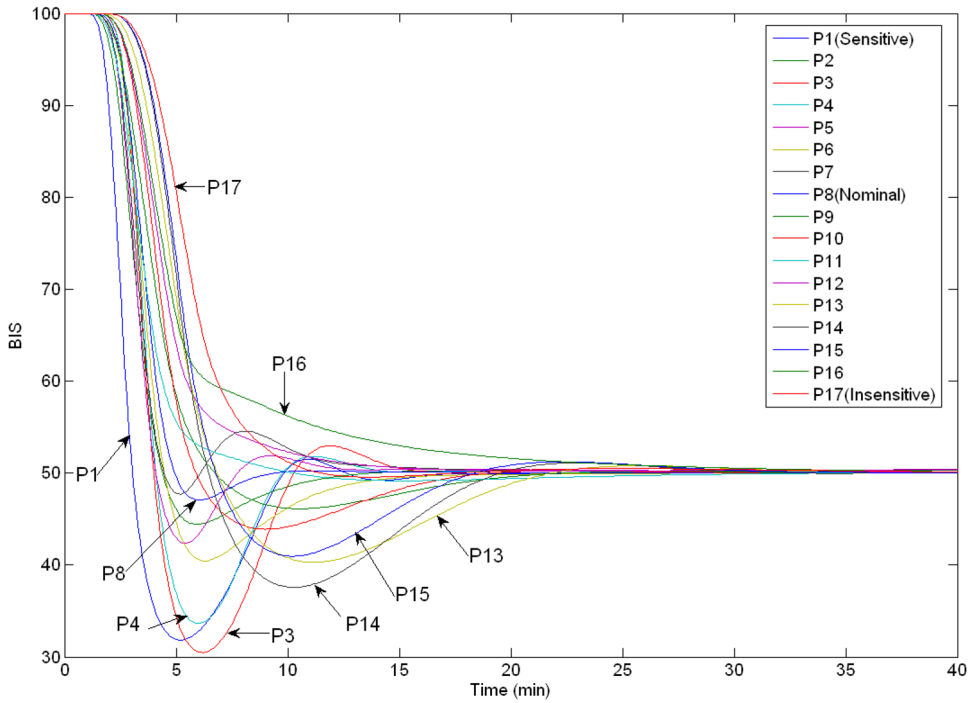

Fig. 9 BIS response with MPC Toolbox controller 40 min into the induction test

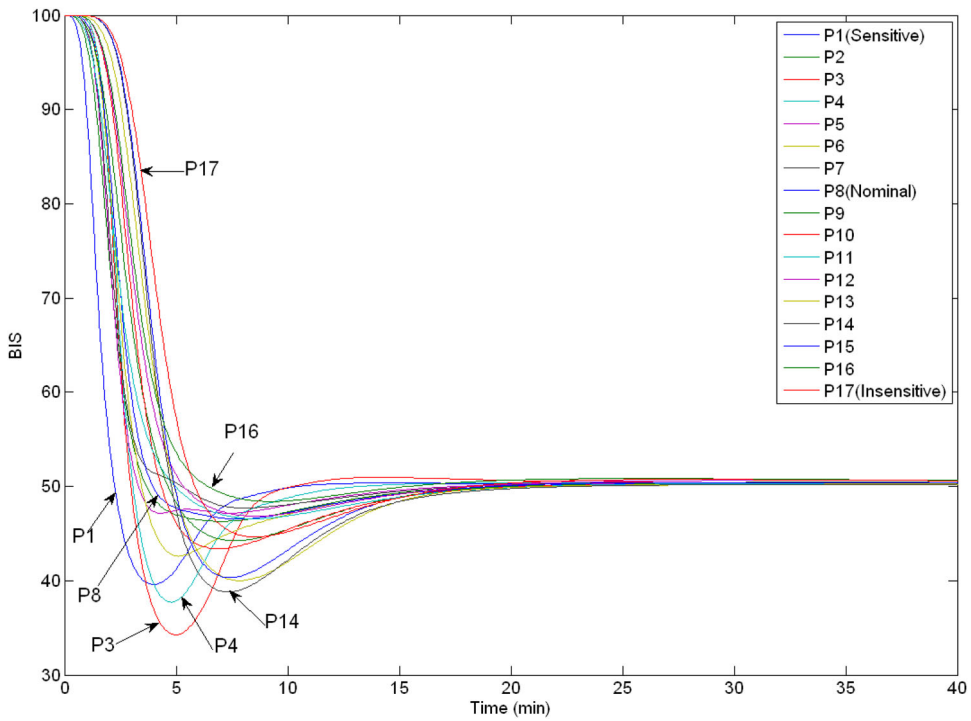

Fig. 10 BIS response with LMPC2 controller 40 min into the induction test

The IAE is mathematically defined as:

$$\text{IAE} = \int_0^t |\in (t)|dt \tag{72}$$

where the error ϵ is the difference between the instantaneous BIS measurement and reference signals.

$$\epsilon = BIS_{measured}(t) - BIS_{reference}(t) \tag{73}$$

3.8 The performance error (PE)

In addition, other statistical indices have appeared in similar works (Ionescu et al., 2008 [10]; Sawaguchi et al., 2008 [8];

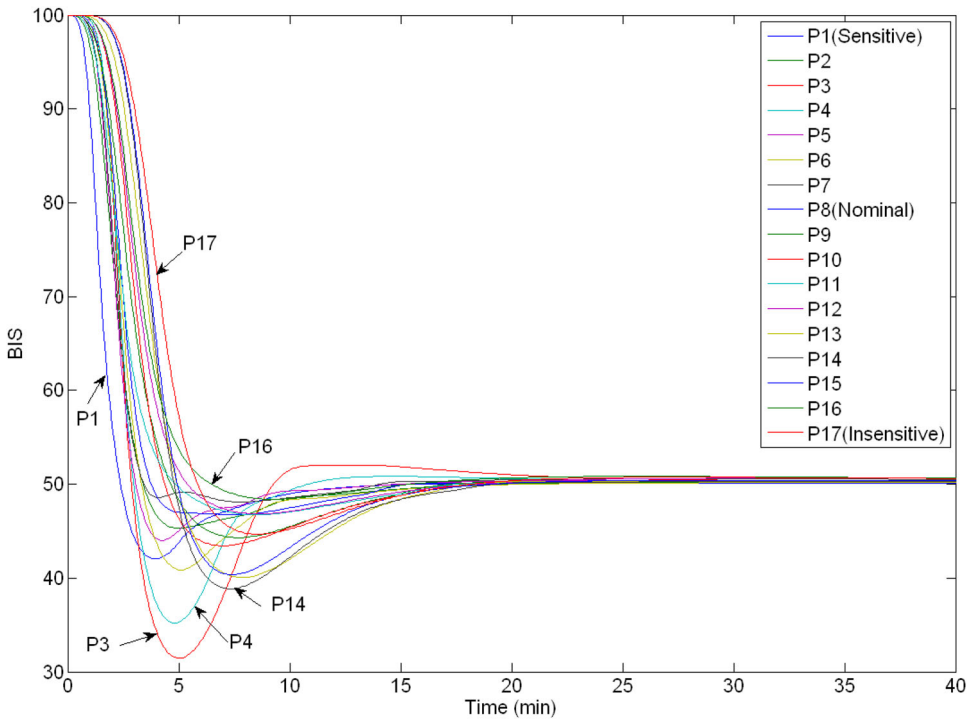

Fig. 11 BIS response with NMPC controller 40 min into the induction test

Moore et al., 2009 [35]; Simanski et al., 2009 [34]; Sreenivas et al., 2009 [33]) that are based on the performance error (PE). The PE is a percentage measure of the deviation from the set point at every time step.

$$PE(t) = \frac{BIS_{measured}(t) - BIS_{reference}(t)}{BIS_{reference}(t)} \times 100\% \quad (74)$$

Expressed for N discrete sampling instants over the anesthesia (simulation) period, Eq. (53) becomes:

$$\boldsymbol{PE(i)} = \frac{\boldsymbol{y_m(i) - r(i)}}{\boldsymbol{r(i)}} \times 100\%; \boldsymbol{i} = 1, 2, \ldots, \boldsymbol{N} \quad (75)$$

where y_m and r refer, respectively, to the measured and reference BIS values.

The following indices are based on the PE.

3.9 Median of the performance error (MDPE)

The MDPE is a measure of control bias defined statistically as the median of the sampled PEs over the anesthesia observation period.

$$MDPE = median[PE(i); i = 1, 2, \ldots, N] \quad (76)$$

It could take negative or positive value and does not give much useful information on the control performance.

3.10 Median of the absolute performance error (MDAPE)

The MDAPE is a measure of control inaccuracy. Unlike the MDPE, it takes only positive values and it indicates the performance of the control system.

$$MDAPE = median[|PE(i)|; i = 1, 2, \ldots, N] \quad (77)$$

Like the IAE, high MDAPE values reflect poor control performance.

3.11 Wobble

Wobble measures the intra-patient variability. It expresses the degree of oscillatory behavior and time-related changes in the output performance [33]. It is mathematically defined as the median of the absolute difference between the PE and MDPE.

$$Wobble = median[|PE(i) - MDPE|; i = 1, 2, \ldots, N] \quad (78)$$

3.12 Input performance index – total variation (TV)

While there are ample output performance indices, not many have been reported in the literature for checking the input moves implemented by anesthetic controllers. For this work,

Table 4 Average performance indices and standard deviation (in bracket) for the induction test

Performance index	Controller			
	PID	LMPC (Toolbox)	LMPC2	NMPC
IAE	232.9 (47.82)	245.9 (54.68)	202.4 (51.09)	194.5 (47.00)
MDAPE	0.5357 (0.2851)	0.2034 (0.1759)	0.5988 (0.2655)	0.6479 (0.2702)
Wobble	0.2954 (0.1454)	0.0839 (0.1012)	0.1078 (0.0909)	0.0658 (0.0522)
Minimum BIS	40.59 (3.480)	42.68 (6.355)	43.24 (4.135)	42.79 (4.618)
TV	39.29 (4.599)	83.72 (3.139)	45.11 (6.620)	49.44 (7.521)

the total variation (TV) [33] defined as the sum of the absolute differences between successive control moves would be utilized.

$$\boldsymbol{TV} = \sum_{\boldsymbol{i}=1}^{\boldsymbol{N}-1} |\boldsymbol{u}(\boldsymbol{i}+1) - \boldsymbol{u}(\boldsymbol{i})|;\ \boldsymbol{i} = 1, 2, \ldots, \boldsymbol{N} \tag{79}$$

TV measures the smoothness of the input. Good control moves are indicated by low values of TV.

3.13 Quantitative evaluation and comparison

The performance error, PE, was computed for all time steps over the 90-min simulation period. The output performance indices IAE, MDAPE, Wobble as well as the input performance index TV were calculated for each of the 17 simulation runs carried out for each controller. Additionally, the least measured value of the BIS during each simulation period was also recorded. This is to aid in assessing the extent of undershoot in the responses.

Table 4 reports the average and standard deviation values of these performance indices for the 17 patient runs for each controller. The NMPC led the controllers in best average performance for the induction tests based on the IAE index. It recorded the least IAE standard deviation of 47 and average of 194.5. However, the MDAPE criterion twists the tide to the favor of the linear MPC Toolbox controller when taken as a measure of control accuracy leaving the NMPC controller as the worst performing. The observed difference might be explained by the MDAPE's use of the median of the lot of values computed for the absolute percentage deviation from the set point over the simulation period (see Eqs. 75 and 77), whereas the IAE integrates the absolute deviation errors over the period (see Eq. 72). The NMPC controller and its corresponding linear counterpart (LMPC2) displayed close performance for some of the patients as they both offered the least integral of the absolute deviations from the set point. This closeness, as earlier established, is not unconnected to the fact that the nonlinear controller exploits the simple computationally friendly structure of the linear controller to build its predictive, optimization and control law frameworks.

They all produced average minimum BIS above 40 to indicate that their average responses to inter-patient variability would sustain patient safety. This is quite desirable. Intra-patient variability is indicated by the Wobble index whose entries in Table 4 also shows that the NMPC returns the best average result for the time-related changes in individual patient output performance.

These induction studies have shown the NMPC strategy to have performed most satisfactorily for the inter-patient and intra-patient variability using the IAE and Wobble as indices. The control moves taken to achieve these, however, ranked next to the worst performance (produced by the MPC Toolbox controller) in the group of four as indicated by the total variation, TV. It is fair therefore to state that there is still room for the improvement for the NMPC algorithm to be able to address the concerns of anesthesia regulation despite its promising results.

4 Conclusion

This article deals with the mathematical design framework of a variety of closed-loop infusion schemes for propofol delivery in general anesthesia which can be deployed to assist clinicians to enhance healthcare delivery during surgical procedures. The main aim of the research is to come up with a better-performing control system which could handle the clinical concerns of automation-based anesthesia and to study the performance of these closed-loop automatic drug infusion patterns via computer simulations prior to actual clinical implementation. Specifically, the design of model predictive control (MPC) strategies and a proportional–integral–derivative (PID) controller were formulated mathematically. The successive linearization technique of MPC was also applied in novelty to anesthesia in this work. It was observed that the MPC control schemes show very great promise for onward clinical adoption for automated drug delivery in anesthesia. The direction for future investigations, as a follow-up on the outcome of this research, would be pseudo-clinical in silico studies which will further test the robustness of the controllers via computer simulations.

Future investigations could also attempt to correlate the performance of the closed-loop infusion systems with the changing patient conditions. Already a framework exists for this as certain population models link PK parameters with mass, height, age and gender of the patients (Niño et al., 2009 [5]; Ionescu et al., 2008 [10]). The result of such correlative investigations could help develop a decision system for the controller. Knowing how a specific patient would "behave" a priori could assist in making the controller "wiser" in predicting control actions.

Acknowledgements The guidance of Prof. Yi Cao is acknowledged during the conduct of the research at Cranfield University. Also, the financial sponsorship of the PTDF Nigeria provided to the author in the form of postgraduate study scholarship is acknowledged.

Author contributions I am the only author.

Funding There was no funding.

Data Availability Not applicable.

Code Availability Not applicable.

Declarations

Conflict of interest I declare that there is no conflict of interest in the publication of this article, and that there is no conflict of interest with any other author or institution for the publication of this article.

Ethical statements I hereby declare that this manuscript is the result of my independent creation under the reviewers' comments. Except for the quoted contents, this manuscript does not contain any research achievements that have been published or written by other individuals or groups. I am the only author of this manuscript. The legal responsibility of this statement shall be borne by me.

References

1. Bequette BW (2003) Process control: modeling, design and simulation. Prentice Hall, New Jersey, USA
2. Nascu, I. and Pistikopoulos, E. N. (2016), Multiparametric model predictive control strategies of the hypnotic component in intravenous anesthesia. In: proceedings of the IEEE international conference on systems, man and cybernetics, October 9–12, 2016, Budapest, Hungary, pp. 2828–2833
3. Nascu I, Krieger A, Ionescu CM, Pistikopoulos EN (2015) Advanced model-based control studies for the induction and maintenance of intravenous anaesthesia. IEEE Trans Biomed Eng 62(3):832–841
4. Krieger A, Pistikopoulos EN (2014) Model predictive control of anesthesia under uncertainty. Comput Chem Eng 71:699–707
5. Niño J, De Keyser R, Syafiie S, Ionescu C, Struys M (2009) EPSAC-controlled anesthesia with online gain adaptation. Int J Adapt Control Signal Process 23(5):455–471
6. Yelneedi S, Samavedham L, Rangaiah GP (2009) Advanced control strategies for the regulation of hypnosis with propofol. Ind Eng Chem Res 48(8):3880–3897
7. Syafiie S, Niño J, Ionescu C, De Keyser R (2009) NMPC for propofol drug dosing during anesthesia induction. In: Magni L, Raimondo DM, Allgöwer F (eds) Nonlinear model predictive control: towards new challenging applications, vol 384. Lecture notes in control and information sciences. Berlin, Heidelberg, pp 501–509
8. Sawaguchi Y, Furutani E, Shirakami G, Araki M, Fukuda K (2008) A model-predictive hypnosis control system under total intravenous anesthesia. IEEE Trans Biomed Eng 55(3):874–887
9. Araki M, Furutani E (2005) Computer control of physiological states of patients under and after surgical operation. Annu Rev Control 29(2):229–236
10. Ionescu CM, Keyser RD, Torrico BC, Smet TD, Struys MMRF, Normey-Rico JE (2008) Robust predictive control strategy applied for propofol dosing using BIS as a controlled variable during anesthesia. IEEE Trans Biomed Eng 55(9):2161–2170
11. Nunes, C. S., Mendonça, T., Lemos, J. M. and Amorim, P. (2007), Control of depth of anesthesia using MUSMAR - exploring electromyography and the analgesic dose as accessible disturbances. In: proceedings of the 29th annual international conference of the IEEE engineering in medicine and biology society, August 23–26, 2007, Lyon, France, pp. 1574–1577
12. Rao RR, Bequette BW, Roy RJ (2000) Simultaneous regulation of hemodynamic and anesthetic states: a simulation study. Ann Biomed Eng 28(1):71–84
13. Nunes, C. S., Mendonça, T., Lemost, J. M. and Amorim, P. (2007), Predictive adaptive control of the bispectral index of the EEG (BIS): Exploring electromyography as an accessible disturbance. In: 2007 Mediterranean conference on control and automation, July 27–29, 2007, Athens, Greece
14. Eskandari N, van Heusden K, Dumont GA (2020) Extended habituating model predictive control of propofol and remifentanil anesthesia. Biomed Signal Process Control 55:101656
15. Savoca A, Manca D (2019) A physiologically-based approach to model-predictive control of anesthesia and analgesia. Biomed Signal Process Control 53:101553
16. Ntouskas S, Sarimveis H (2021) A robust model predictive control framework for the regulation of anesthesia process with Propofol. Optim Control Appl Methods 42(4):965–986
17. Copot, D., Kusse, F., Ghita, M., Ghita, M., Neckebroek, M., & Maxim, A. (2019). Distributed model predictive control for hypnosis-hemodynamic maintenance during anesthesia. In: 2019 23rd international conference on system theory, control and computing (ICSTCC) (pp. 638–643). IEEE
18. Maxim A, Copot D (2021) Closed-loop control of anesthesia and hemodynamic system: a model predictive control approach. IFAC-PapersOnLine 54(15):37–42
19. Adhau, S., Patil, S., Ingole, D., & Sonawane, D. (2019). Embedded implementation of deep learning-based linear model predictive control. In: 2019 sixth Indian control conference (ICC) (pp. 200–205). IEEE
20. Copot, D., & Maxim, A. (2019). Model predictive control for simultaneous regulation of hypnosis and hemodynamic states. In: 2019 18th European control conference (ECC) (pp. 4106–4111). IEEE
21. Jing CJ, Syafiie S (2021) Multi-model generalised predictive control for intravenous anaesthesia under inter-individual variability. J Clin Monit Comput 35(5):1037–1045
22. Savoca A, Barazzetta J, Pesenti G, Manca D (2018) Model predictive control for automated anesthesia. Comput Aid Chem Eng 43:1631–1636
23. Hosseinzadeh M, van Heusden K, Yousefi M, Dumont GA, Garone E (2020) Safety enforcement in closed-loop anesthesia—a comparison study. Control Eng Practice 105:104653
24. Bequette BW, Doyle FJ (2001) Automated control in biomedicine. IEEE Eng Med Biol Mag 20(1):22–23

25. Bickford RG (1950) Automatic electroencephalographic control of general anesthesia. Electroencephalogr Clin Neurophysiol 2(1–4):93–96
26. Beck C, Lin H-H, Bloom M (2007) Modeling and control of anesthetic pharmacodynamics. In: Queinnec I, Tarbouriech S, Garcia G, Niculescu S-I (eds) Biology and control theory: current challenges, vol 357. Lecture notes in control and information sciences. Berlin, Heidelberg, pp 263–289
27. Marsh B, White M, Morton N, Kenny GNC (1991) Pharmacokinetic model driven infusion of propofol in children. Br J Anaesth 67(1):41–48
28. Oshin TA (2016) Automation in anaesthesia. Lambert Academic Publishing, Saarbrucken, Germany
29. The MathWorks (2004), Model Predictive Control Toolbox^{TM} User's Guide, Version 2.0, The MathWorks Inc., USA
30. Al Seyab RK, Cao Y (2006) Nonlinear model predictive control for the ALSTOM gasifier. J Process Control 16(8):795–808
31. Rossiter JA (2003) Model-based predictive control: a practical approach. CRC Press, Boca Raton, Florida, USA
32. Rowe WL (1998) Economics and anaesthesia. Anaesthesia 53:782–788
33. Sreenivas Y, Yeng TW, Rangaiah GP, Lakshminarayanan S (2009) A comprehensive evaluation of PID, cascade, model-predictive, and RTDA controllers for regulation of hypnosis. Ind Eng Chem Res 48(12):5719–5730
34. Simanski O, Janda M, Schubert A, Bajorat J, Hofmockel R, Lampe B (2009) Progress of automatic drug delivery in anaesthesia-the "Rostock assistant system for anaesthesia control (RAN)." Int J Adapt Control Signal Process 23(5):504–521
35. Moore, B. L., Pyeatt, L. D. and Doufas, A. G. (2009), Fuzzy control for closed-loop, patient-specific hypnosis in intraoperative patients: a simulation study. In: proceedings of the 31st annual international conference of the IEEE engineering in medicine and biology society, September 2–6, 2009, Minneapolis, Minnesota, USA, pp. 3083–3086